Charge transfer into the metastable 2S level of hydrogen by protons colliding with K and Na

J. K. Berkowitz* and Jens C. Zorn
Physics Department, The University of Michigan, Ann Arbor, Michigan 48109
(Received 13 May 1983)

We measure the charge transfer cross section for protons in potassium and sodium with the final state being $H(2s)+A^+$. Using a crossed-beam experimental method we look at this cross section as a function of proton beam energy from 500 to 2500 eV. Our results for potassium agree with previous experiments and theories in showing two main peaks in the cross section: one of $(3.9\pm1.5)\times10^{-15}$ cm^2 at a proton beam energy of 800 eV, and another of $(2.8\pm1.1)\times10^{-15}$ cm^2 at a proton beam energy of 2.5 keV. Our results for sodium show a steadily rising cross section with a value of $(7.3\pm2.5)\times10^{-15}$ cm^2 at a proton beam energy of 2.5 keV in agreement with the prediction of Kubach and Sidis; we do not find the maximum at 700 eV reported by Nagata that agrees with the theory of Kimura, Olson, and Pascale.

I. INTRODUCTION

Ion-atom charge transfer collisions are of great interest both theoretically and experimentally. Hasted[1] gives an excellent general review of the field. We are concerned with a specific family of charge transfer collisions, that of charge pickup by hydrogen ions (protons) in metal vapors. Alverez and Cisneros[2] and Brouillard[3] review the experimental and theoretical portions of this area of charge transfer collisions. Neutralization of H^+ is of interest in the area of plasma fusion as a method of energetic neutral beam injection into fusion reactors. At lower energies, this charge exchange process is used to make metastable [$H(2s)$] hydrogen used for atomic experiments[4–6] and for the creation of spin polarized proton beams for injection into large accelerators.[7,8]

The energy difference ("energy defect") between the ionization energy of alkali-metal atoms and the energy of the $n=2$ level in atomic hydrogen ranges from 0.5 eV in cesium to 2 eV in lithium. This relatively small energy defect causes near resonant conditions for charge transfer collisions of the form

$$A+H^+\rightarrow A^++H(2s)\ ,$$

where A represents the alkali-metal atom. Most of the attention, both theoretical and experimental, has been focused on the collision of protons with cesium,[9,10] with the lighter alkali metals receiving some recent experimental[11,12] and theoretical[13,14] attention. It is notable that the reasonable agreement found among the investigations in cesium, rubidium, and potassium does not extend to sodium, where contradictory theories, and now contradictory experiments exist, nor to lithium where experiments and theory remain to be done.

II. THEORETICAL CONSIDERATIONS

The customary theoretical approach used for the description of relatively low-energy (<10 keV) charge exchange collision processes

$$A+B^+\rightarrow A^++B \tag{1}$$

involves treating the system $(A\text{-}B)^+$ as a quasimolecule. The energies and wave functions of the molecular states associated with the two channels of interest (A^+-B and A-B^+) are then calculated. The charge exchange matrix element $\langle A^+B\,|\,H_{12}\,|\,AB^+\rangle$ is then determined where H_{12} is the coupling mechanism. In the specific case of interest where B is a hydrogen atom and A is an alkali-metal atom, the quasimolecular states for the interaction

$$H^++A\rightarrow H(n=2)+(A)^+ \tag{2}$$

can be approximated as those of an electron in the field of two ionic cores.[13–16]

Kubach and Sidis[13] use a perturbed stationary state approach to the problem. With a projected valence bond expansion of the eigenstates, and with a numerical Hartree-Fock potential for the alkali-metal ion core, they calculate the charge exchange elements of the scattering matrix. This approach leads to diabatic mixing in which level crossing is allowed. The calculation by Kubach and Sidis yields the total cross section for charge exchange into the $n=2$ state of hydrogen: $Q_{CE}(2s+2p)$. To obtain $Q_{CE}(2s)$, the cross section for production of $2s$ hydrogen, from $Q_{CE}(2s+2p)$ they look at secondary long-range sharing processes with a calculation that, although done explicitly for cesium, should be quite similar for all the alkali metals. For purposes of comparing our experiment to the Kubach and Sidis theory, however, we use an experimental measurement[12] of the ratio $Q_{CE}(2s)/Q_{CE}(2s+2p)\equiv f_{2s}$ for the curves shown in Fig. 1. (This experimental value for f_{2s} varies no more than 15% from Sidis and Kubach's theoretical cesium f_{2s} prediction.)

Kimura, Olson, and Pascale[14] also use a molecular state expansion of the wave function in order to calculate $Q_{CE}(2s)$ directly. They expand the wave functions necessary to solve the time-dependent Schrödinger equation in Slater-type atomic orbitals without the orthogonalization used by Kubach and Sidis; this leads to adiabatic mixing. It should be mentioned that Kimura *et al.* use an analytic

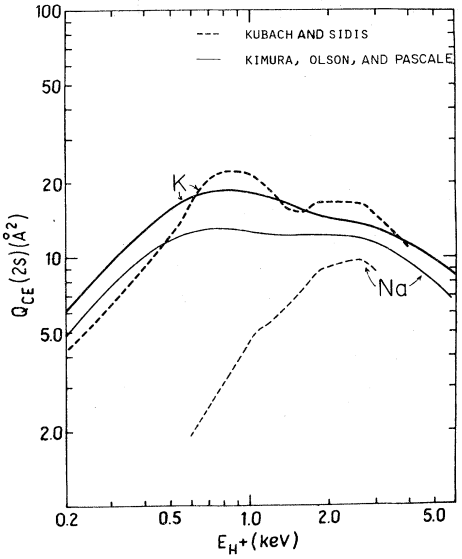

FIG. 1. Calculated values of $Q_{CE}(2s)$ vs E_{H^+} by Kubach and Sidis (Ref. 13) (dashed lines) and Kimura, Olson, and Pascale (Ref. 14) (solid lines), for potassium (thick lines) and sodium (thin lines).

pseudopotential which has been adjusted to fit spectroscopic data to represent the potential of the alkali-metal atom core. They write their time-dependent wave function as

$$\psi(\vec{r},t)=\sum_i a_j(t)\phi_i(\vec{r},R)F_i(r,R)\ ,$$

where ϕ_i are the time-independent wave functions; the F_i are factors that account for the translational motion of the ionic cores which leads to diabatic coupling of the wave functions. The predictions by Kimura, Olson, and Pascale for $Q_{CE}(2s)$ for K and Na targets are shown in Fig. 1.

III. EXPERIMENTAL APPARATUS

The apparatus produces a beam of protons of known energy that collide with a thin target of alkali-metal atoms whose density is known; the number of excited, metastable hydrogen atoms that are formed in the proton—alkali-metal collision is then counted. A schematic of the apparatus is shown in Fig. 2. Oil diffusion pumps with water-cooled baffles and liquid-nitrogen traps provide a base pressure of 2×10^{-7} Torr in the system. In full operation the pressures rise to 3×10^{-5} Torr in the source chamber and 1×10^{-6} in the interaction chamber due to the gas loads from the proton source and alkali-metal atom source, respectively, while the detector chamber remains at the base pressure.

The source chamber contains a Colutron model 100 ion source[17] that operates with a 200-mA dc arc to provide about 3 μA of ions. The ions then pass through accelerating and focusing electrodes in an Einzel lens configuration that permits one to alter the proton energy without having to refocus the beam.

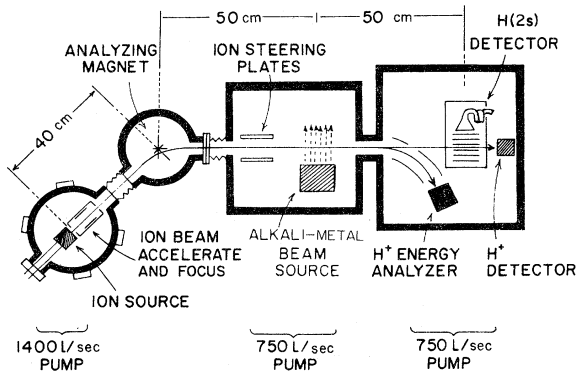

FIG. 2. Experimental apparatus schematic.

The ion beam passes from the source chamber to a magnetic field ($\sim$100 g) for momentum analysis. This discriminates strongly against ions other than protons, and provides a $\pm$20-eV energy resolution for beam energies over the range 500—2500 eV. The lower energy limit of this experiment is set by the difficulty of maintaining a proton beam of adequate intensity and stability at energies below 500 eV. The upper energy of the proton beam is limited because the ion source requires high-current power supplies that float at ion beam accelerating voltage. The insulation within the power supplies that were available to us break down at voltages above 2500 V.

The interaction chamber contains a set of steering plates, a movable Faraday cup to measure the ion current immediately before the interaction region, an alkali-metal oven, and a liquid-nitrogen—cooled shield which defines the interaction region and collects the alkali-metal beam. Figure 3 shows a perspective drawing of the oven-interaction region assembly. The oven is constructed of stainless steel and has 15 exit channels, each of which is 2.2 cm long and has a square cross section of 0.13×0.13 cm; the separation between adjacent channels is 0.05 cm. The oven is electrically heated in a manner which maintains the exit channels about 25 K above the alkali-metal reservoir.

The alkali-metal beams from the oven exit channels rise vertically into a region that is defined by the cold ($\sim$100 K), copper cylindrical shield that traps alkali-metal atoms with good efficiency; two 0.75-cm-diam tubes in the sides of this cylinder provide for the entrance and exit of the proton beam 2.9 cm distant from the top of the oven. It is within this 0.75-cm-diam, 3.4-cm-long cylindrical region inside the cold shield that the proton—alkali-metal collisions takes place.

After leaving the interaction region the beam, which now has three constituents (protons, fast ground-state hydrogen atoms, and a small proportion of fast metastable hydrogen atoms), enters the detection chamber. This chamber contains a set of curved electrostatic deflection plates which allows us to measure the absolute proton beam energy, a metastable detection region, and a Faraday cup to measure the proton beam intensity.

Fast hydrogen atoms in the metastable $2\,^2S_{1/2}$ state are detected by counting the Lyman-α photons that are emitted when they enter a dc electric field. The intrinsic life-

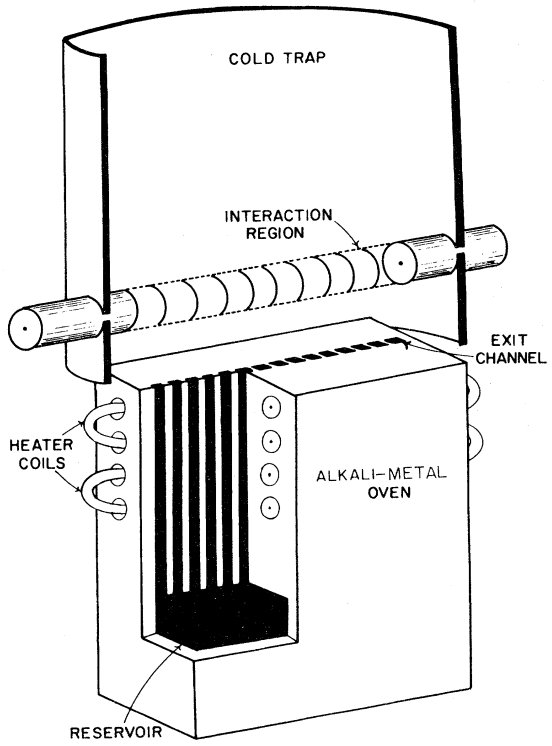

FIG. 3. Cutaway perspective of the alkali-metal oven-interaction region.

time of the metastable state is more than 0.1 sec, but the application of an electric field of strength E admixes $2p$ components to the wave function which in turn reduces the lifetime to $3.6\times10^{-4}/E^2$ sec.[18] In this experiment, a field of 160 V/cm (in which the lifetime of the metastable atom is only 14 nsec) is applied over a 5 cm length of the beam, and this quenches more than 90% of the metastable atoms within the view of an electron multiplier.

The continuous channel electron multiplier used for detection of the 1216-Å Lyman-α photons is mounted behind a MgF_2 window and inside a metal box in order to minimize spurious detector signals from the proton beam. The window itself is covered with a fine, highly transparent gold mesh that prevents static charge buildup on the window from significantly affecting the electric fields in the quench region. Owing to limitations in solid angle (0.5 sr), MgF_2 window transmission (0.35), and detector quantum efficiency (0.02) our H($2s$) detector has an efficiency of only 3×10^{-4}. Nevertheless, given the low noise of the detector (<6 counts/sec) and reasonable metastable production rate ($\sim10^7$/sec), this small detector efficiency does not lead to unreasonable integration times for a data run.

Under typical conditions, a 1.5-keV proton beam of 2×10^{-8} A passing through an alkali-metal target yields about 4000 metastable atom counts/sec, about 200 of which are from metastable atoms formed when protons pick up electrons from the background gas in the interaction or detection chambers.

IV. PROCEDURE

The ion source requires about 2 h to achieve equilibrium in temperature, gas flow, and discharge current before an adequately stable proton beam becomes available. During the ion source warmup time, the metastable detector is used to determine the background level of H($2s$) atoms that are formed when a proton picks up an electron from molecules in the $\sim3\times10^{-7}$ Torr background gas.

The alkali-metal oven is then slowly heated to operating temperature over a span of a few hours to melt the alkali metal slowly and thereby avoid the sputtering of residual alkali-metal hydroxides which can block the entrance channels. This gradual heating also allows for a slow and thorough outgassing of the oven; to keep background gases to a minimum, the oven is briefly heated to 50° above the operating temperature before the temperature is stabilized at typical values of 477 K for potassium or 558 K for sodium. The temperature of the oven is carefully monitored and stabilized to within ±0.5 °C.

After the proton and alkali-metal beams have stabilized, the data taking begins by setting the overall ion source potential and determining the peak proton energy and the proton beam energy width. The energy width of the proton beam is determined by applying a stopping potential to an aperture in front of the metastable atom detector. There is about 40 V difference between the potential that still allows 90% of the protons to get through and the potential that allows only 10% to pass, and we conclude that the characteristic energy width of the proton beam in our apparatus is ±20 eV. To determine the beam energy, we apply an appropriate voltage to a set of curved deflecting plates so that the proton component of the beam is deflected into an auxiliary Faraday cup; a measurement of the deflection voltage together with a knowledge of the deflection plate geometry permits the peak proton energy to be determined within ±8 eV.

The number of metastable atoms counted over a 300-sec interval is then recorded along with the proton flux and the oven temperature for the same time interval. The proton energy is then verified before changing the ion source potential and repeating the process for the next data point. About 20 such points, taken at 100-eV intervals, comprise a run.

V. DATA ANALYSIS

A. Determination of the cross section

The metastable count rate (N) depends linearly on the proton beam current (I^+), the efficiency of the metastable atom detector (ϵ), the alkali-metal atom target thickness (τ), and the charge transfer cross section (Q_{CE}). Thus we can write

$$Q_{CE}=\frac{N}{I^+\tau\epsilon}\ .$$

N and I^+ are directly measured rates (see Sec. IV) while ϵ can be calculated from known values for the transparency of the MgF_2 window, the quantum efficiency for Lyman-α photons of the electron multiplier, and the physical di-

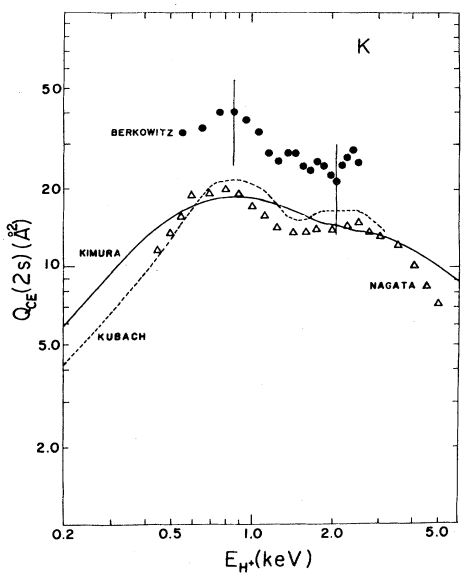

FIG. 4. Experimental results and theoretical predictions in potassium. Solid line, theory of Kimura *et al.* (Ref. 14); dashed line, theory of Kubach and Sidis (Ref. 13); triangles, experimental results of Nagata (Ref. 12); solid circles, present work. Error bars on our results represent the uncertainty in the absolute cross-section measurement. This error is due mainly to the uncertainty in the alkali-metal target thickness. Relative uncertainty in our results would be represented by error bars which are smaller than the circles in the figure that represent them.

mensions of the metastable detector region.

We calculate the thickness of the alkali-metal atom target by using the equations that describe the flow of real gases under the conditions and geometry of our experiment. Atoms within the alkali-metal oven reservoir have a mean free path that is somewhat smaller than the width of the oven channels, but as they progress through the channel to regions of lower pressure, atom-atom collisions become less likely than collisions with the walls. Eventually the atoms get to a region within the channel where the mean free path for atom-atom collisions equals the remaining length of the channel.

The relationship between the pressure within the reservoir and the pressure within the channel in the transition region can be calculated from the equations that govern noneffusive flow[19] since we know the viscosity of the gas and the temperature of the vapor. The pressure within and location of this transition region then govern the flow rate and angular distribution of alkali-metal atoms from the channel exit in a manner that can be calculated from the equations of effusive flow[19,20] from long tubes.

The mean free path of an alkali-metal atom as it leaves the exit channel is greater than the distance from the oven exit to the cold trap that collects the atom after it has passed through the interaction region. Therefore atom-atom collisions in the alkali-metal beam can be neglected.

After the total flow rate and angular distribution of each of the alkali-metal beams is calculated, an integration over the interaction region gives the total number of target atoms from each of the channels. The target thickness is calculated by summing the contributions from each channel and then dividing by the cross-sectional area of the interaction region as seen by the proton beam.

B. Uncertainty and error

The uncertainty in our results that arises from statistical fluctuations and background is relatively small ($\pm 3\%$) since the instability of the beams and the noise of the detectors can be overcome by integrating for a sufficient length of time for all but the data below 800 eV in sodium. The principle sources of systematic error are uncertainties in the thickness of the alkali-metal atom target and the efficiency of the metastable atom detector.

The numerical value of the target thickness is quite sensitive to the value used for the coefficient of viscosity (η). A small shift in the value of viscosity will change the calculated value of the mean free path. Such shifts will affect not only the calculated flow rates but also the calculated location of the transition region in the oven channel which governs the angular distribution of atoms as they leave the channels. The uncertainty of 10% from the nominal values of η given by Stefanov[21] leads to an uncertainty in our estimate of target thickness of 33%.

The likelihood of detecting metastable H($2s$) atoms depends linearly on the probability of quenching the atom within the detector ($0.90\pm 5\%$), the solid angle subtended by the uv-sensitive multiplier ($4.7\times 10^{-2}\pm 10\%$), the transmission of the window for Lyman-α radiation ($0.35\pm 15\%$), and the quantum efficiency of the channeltron for Lyman-α radiation ($2\times 10^{-2}\pm 10\%$). This leads to a total uncertainty in the metastable detector efficiency of 21%.

We conclude that (with the exception of data below 800 eV in sodium where low count rates led to significant statistical errors) the absolute values of cross section reported in this work are accurate to within $\pm 40\%$. For the two data points in sodium below 800 eV (750 and 650 eV) the statistical error in the count rate leads to total uncertainties of $\pm 43\%$ and $\pm 54\%$, respectively.

VI. RESULTS AND CONCLUSIONS

Figure 4 shows experimental results and theoretical predictions for electron exchange into the final H($2s$) states from the ($4s$) state of potassium as a function of proton beam energy. The theoretical predictions of Kubach and Sidis[13] and that of Kimura *et al.*[14] are in good agreement, with differences of less than 15% between 600 eV and 3 keV proton beam energy. The experimental results presented in Fig. 4 [Nagata, Ref. 12(c) and our values] are also in reasonable agreement with each other and with the theories.

For sodium, however, the situation is less satisfactory. Figure 5 shows the H^+ energy dependence of the experimental results and theoretical predictions of the cross section for the process $H^+ + Na(3s) \rightarrow H(2s) + Na^+$. The authors and their papers are the same as in Fig. 4. For H^+ beam energies below 3 keV, there is a significant diver-

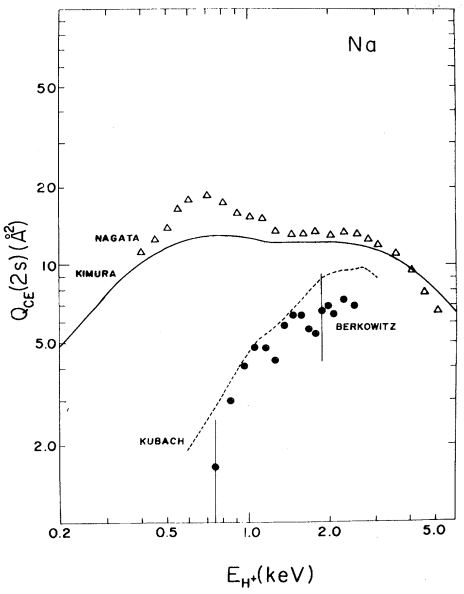

FIG. 5. Experimental results and theoretical predictions in sodium. Solid line, theory of Kimura *et al.* (Ref. 14); dashed line, theory of Kubach and Sidis (Ref. 13); triangles, experimental results of Nagata (Ref. 12); solid circles, present work. Error bars on our results represent the uncertainty in the absolute cross-section measurement. This error is due mainly to the uncertainty in the alkali-metal target thickness. Relative uncertainty in our results would be represented by error bars which are smaller than the circles in the figure that represent them.

gence between theories and between experiments.

Prior to 1980, the status of the work done in sodium was that the experimental results by Nagata[12] were in disagreement with the calculation done by Kubach and Sidis. Motivated by the disagreement, we undertook this experiment. In the meantime, however, Kimura, Olson, and Pascale[14] completed their calculation which disagreed with the earlier calculation and supported the Nagata experimental results. We cannot suggest which theoretical approach should take precedence since the models are complex and the calculations intricate, but our measurements support the theoretical result of Kubach and Sidis.

The two experiments differ in the nature of their interaction regions. Nagata[12] employs a hot vapor cell in which the atoms move randomly as in a gas, and the density of that gas is determined by using a surface ionization detector to measure the flux of atoms that leave the cell through a small hole in the top. However, the efficiency of surface ionization detectors is very (and often erratically) dependent on the temperature and conditions of the ionizing surface. This is particularly true for atoms such as sodium where the work function of the surface barely exceeds the ionization potential of the atom.

Errors in the determination of target thickness are a frequent concomitant of absolute cross-section determinations, of course, and they may account for the difference between the two experimental results for potassium. Such errors would not explain why the two experiments yield such different results for the energy dependence of the cross section in sodium. It is possible that an unexpectedly high concentration of alkali-metal dimers and trimers[22] in a vapor target might lead to such differences because the larger number of energy levels in a molecule gives more opportunity at low energies for resonant charge transfer, but our estimates suggest that the concentration of dimers and higher polymers is too low to explain the difference between the experiments. Another possibility, suggested independently by Nagata[23] and by others in private communications, is that even a small amount of impurity in the sodium oven load can lead to large systematic errors if that impurity (potassium, for example) has a high vapor pressure at the 550 K oven temperature that is typical for an experiment with sodium.

The previous experimental and theoretical results for charge exchange seem to be in good agreement for the heavier alkali-metals (Cs,Rb,K). The disagreements for sodium, the lightest alkali metal for which there are both experimental results and theoretical predictions, are troublesome. An experiment and theoretical prediction in lithium, the lightest alkali metal, would be useful in determining whether the discrepancies seen in Na are due to experimental techniques, an incomplete theory, or both.

ACKNOWLEDGMENTS

This research was supported in part by the National Science Foundation under Grant No. PHY-77-18832. We thank Professor W. L. Williams and Professor C. E. Wieman for their help, particularly in the first phases of this work.

*Present address: Lighting Products Group, GTE/Sylvania Lighting Center, Danvers, MA 01923.

[1]J. B. Hasted, Adv. At. Mol. Phys. 15, 205 (1979).
[2]I. Alvarez T. and C. Cisneros G., Rev. Mex. Fis. 27, 179 (1981).
[3]F. Brouillard, Phys. Scr. 23, 163 (1981).
[4]R. R. Lewis and W. L. Williams, Phys. Rev. Lett. 59B, 70 (1975).
[5]E. A. Hinds and V. W. Hughes, Phys. Lett. 67B, 487 (1977); E. A. Hinds, Phys. Rev. 44, 374 (1980).
[6]E. G. Adelberger *et al.*, Nucl. Instrum. Methods 179, 181 (1981).
[7]T. Trainor, Ph.D. thesis, University of North Carolina, 1973 (available from University Microfilms, Ann Arbor, Michigan).
[8]G. P. Lawrence, G. G. Ohlsen, and J. L. McKibben, Phys. Lett. 28B, 594 (1969).
[9]R. E. Olson, E. J. Shipsey, and J. C. Browne, Phys. Rev. A 13, 1 (1976).
[10]B. L. Donnally, T. Clapp, W. Sawyer, and M. Schultz, Phys. Rev. Lett. 12, 502 (1964).
[11]W. Gruebler, P. A. Schmelzbach, V. Konig, and P. Marmier, Helv. Phys. Acta 43, 254 (1970).
[12](a) T. Nagata, J. Phys. Soc. Jpn. 46, 919 (1979); (b) 46, 1622 (1979); (c) in *XIth Conference on the Physics of Electronic and Atomic Collisions, 1979,* edited by K. Takayanagi and N. Oda (North-Holland, Amsterdam, 1980), p. 512.

[13]C. Kubach and V. Sidis, Phys. Rev. A 23, 110 (1981); J. Phys. B 11, 2687 (1978).
[14]M. Kimura, R. E. Olson, and J. Pascale, Phys. Rev. A 26, 3113 (1982).
[15]A. Valence and G. Spiess, J. Chem. Phys. 63, 1487 (1975).
[16]R. E. Olson, F. T. Smith, and E. Bauer, Appl. Opt. 10, 8 (1971).
[17]M. Menzinger and L. Wahlin, RSI 40, 102 (1969).
[18]H. A. Bethe and E. E. Salpeter, *Quantum Mechanics of One- and Two- Electron Atoms,* 1st ed. (Springer, Berlin, 1957).
[19]J. Berkowitz, Ph.D. thesis, University of Michigan, 1983 (available from University Microfilms, Ann Arbor, Michigan).
[20]J. A. Giordmaine and T. C. Wang, J. Appl. Phys. 31, 463 (1960).
[21]Boris Stefanov, High Temp. High Pressures 12, 189 (1980).
[22]M. Lambropoulos and S. E. Moody, Rev. Sci. Instrum. 48, 2 (1977).
[23](a) T. Nagata, Mass Spectrosc. 30, 153 (1982); (b) J. Phys. Soc. Jpn. 52, 4 (1983). The latter paper gives a report of a crossed-beam proton-cesium experiment.